Brochon, J. C., Wahl, P., & Auchet, J. C. (1974) *Eur. J. Biochem. 41*, 577–583.
Cotton, F. A., & Hazen, E. E., Jr. (1971) *Enzymes (3rd Ed.) 4*, 153–175.
Eftink, M. R., & Ghiron, C. A. (1987) *Biophys. J. 52*, 467–473.
Eftink, M. R., Ghiron, C. A., Kautz, R. A., & Fox, R. O. (1989) *Biophys. J. 55*, 575–579.
Eftink, M. R., Ghiron, C. A., Kautz, R. A., & Fox, R. O. (1990) *Proc. SPIE–Int. Soc. Opt. Eng. 1204*, 137–143.
Eftink, M. R., Gryczynski, I., Wiczk, W., Laczko, G., & Lakowicz, J. R. (1991) *Biophys. Chem.* (submitted for publication).
Evans, P. A., Dobson, C. M., Kautz, R. A., Hatfull, G., & Fox, R. O. (1987) *Nature 329*, 266–268.
Fox, R. O., Evans, P. A., & Dobson, C. A. (1986) *Nature 320*, 192–194.
Grinvald, A., & Steinberg, I. Z. (1976) *Biochim. Biophys. Acta 27*, 663–678.
Hansen, D., Altschmied, L., & Hillen, W. (1987) *J. Biol. Chem. 262*, 14030–14035.
Hudson, B., Ruggiero, A., Harris, D., Johnson, T., Dou, X. M., Novet, T., McIntosh, L., Phillips, C., & Nester, T. (1988) *Proc. SPIE-Int. Soc. Opt. Eng. 909*, 113–120.
Hynes, T. R., Kautz, R. A., Goodman, M. A., Gill, J. F., Fox, R. (1989) *Nature 339*, 73–76.
Kautz, R. A., Gill, J. F., & Fox, R. O. (1990) in *Protein and Pharmaceutical Engineering*, pp 1–15, Wiley-Liss, Inc., New York.
Kellis, J. T., Jr., Nyberg, K., Sali, & Fersht, A. R. (1988) *Nature 333*, 784–786.
Kitamura, S., & Sturtevant, J. M. (1989) *Biochemistry 28*, 3788–3792.
Lakowicz, J. R., Laczko, G., Gryczynski, I., & Cherek, H. (1986) *J. Biol. Chem. 261*, 2240–2245.
Matsumura, M., Becktel, W. J., & Matthews, B. W. (1988) *Nature 334*, 406–410.
Matthews, B. (1987) *Biochemistry 26*, 6885–6888.
Matthews, B. W., Nicholson, H., & Becktel, W. J. (1987) *Proc. Natl. Acad. Sci. U.S.A.*
Oxender, D. L., & Fox, C. F. (1987) *Protein Engineering*, Alan R. Liss, Inc., New York.
Pace, C. N., Shirley, B. A., & Thomson, J. A. (1989) in *Protein Structure and Function: A Practical Approach* (Creighton, T. E., Ed.) pp 311–330, IRL Press, Oxford, England.
Schellman, J. A. (1978) *Biopolymers 17*, 1305.
Serpersu, E. H., McCracken, J., Peisach, J., & Mildvan, A. S. (1988) *Biochemistry 27*, 8034–8044.
Shortle, D., & Meeker, A. K. (1986) *Proteins: Struct., Funct., Genet. 1*, 81–89.
Shortle, D., Meeker, A. K., & Freire, E. (1988) *Biochemistry 27*, 4761–4768.
Waldman, A. D. B., Clarke, A. R., Wigley, D. G., Hart, K. W., Chia, W. N., Barstow, D., Atkinson, T., Munro, I., & Holbrook, J. J. (1987) *Biochim. Biophys. Acta 913*, 66–71.
Weaver, L. A., Gray, T. M., Grutter, M. G., Anderson, D. E., Wozniak, J. A., Dahlquist, F. W., & Matthews, B. W. (1989) *Biochemistry 28*, 3793–3797.
Zipp, A., & Kauzmann, W. (1973) *Biochemistry 12*, 4217–4228.

Internal Intensity Standards for Heme Protein UV Resonance Raman Studies: Excitation Profiles of Cacodylic Acid and Sodium Selenate†

Sunho Song and Sanford A. Asher*
Department of Chemistry, University of Pittsburgh, Pittsburgh, Pennsylvania 15260
Received July 18, 1990; Revised Manuscript Received October 9, 1990

ABSTRACT: We examine the utility of SO_4^{2-}, ClO_4^-, cacodylic acid, and SeO_4^{2-} as internal intensity standards for Raman spectral measurements of protein structure. We find that 0.1 M SO_4^{2-} and ClO_4^- perturb the protein tertiary structure of aquomethemoglobin (met-Hb) and its fluoride (met-HbF) and azide (met-HbN_3) complexes. Changes occur for the tryptophan near-UV absorption bands, the iron spin state is altered, and the fluoride ligand affinity decreases. Concentrations of ClO_4^- and SO_4^{2-} as low as 0.1 M suppress the met-HbF quaternary R → T transition induced by the allosteric effector inositol hexaphosphate (IHP). In contrast, similar concentrations of cacodylic acid and SeO_4^{2-} show little effect on the hemoglobin tertiary or quaternary protein structures or upon the R → T transition induced by IHP. We measure the Raman cross sections of cacodylic acid and SeO_4^{2-} between 218 and 514.5 nm and find that for UV excitation they are ca. 5-fold larger than ClO_4^- or SO_4^{2-}. Thus, cacodylic acid and selenate can be used at lower concentrations. Cacodylic acid and SeO_4^{2-} are superior Raman internal intensity standards for protein structural studies.

The use of resonance Raman spectroscopy for biomolecular studies has recently been extended into the UV region in order to probe aromatic chromphores such as aromatic amino acids in proteins and nucleic acid bases (Asher, 1988). For example, recent applications have included studies of tyrosine and tryptophan in hemoglobin (Song & Asher, 1990; Asher, 1988; Kaminaka et al., 1990; Su et al., 1989), in myoglobin (Harmon et al., 1990; Larkin et al., 1990a), and in bacteriorhodopsin (Harada et al., 1990) as well as other proteins [see Sweeney et al. (1990), Asher (1988), and Harada and Takeuchi (1986) and references cited therein]. In these studies, significant environmental information derives from the Raman intensities. The intensity information is generally obtained from Raman

† This work was supported by NIH Grant IR01GM30741-09.
* Author to whom correspondence should be addressed.

0006-2960/91/0430-1199$02.50/0

measurements which use internal intensity standards contained within the sample (Dudik et al., 1985; Blazej & Peticolas, 1980a,b; Trulson & Mathies, 1986; Li & Myers, 1990). This is crucial because the internal standards allow the experimenter to avoid notoriously difficult absolute intensity measurements (Larkin et al., 1990b).

A number of Raman excitation profile studies have recently been reported for molecular species useful as Raman internal standards for aqueous solution studies (Dudik et al., 1985; Blazej & Peticolas, 1980a,b; Trulson & Mathies, 1986; Kubasek et al., 1985; Li & Myers, 1990). These have included ClO_4^-, NO_3^-, and SO_4^{2-} (Dudik et al., 1985). The ideal internal intensity standard would be useful at low concentrations, and would not interact with the biomolecular analyte, for example, to change the protein structure or activity. In addition, the internal standard should not be photochemically active or significantly absorb the excitation or Raman scattered light.

In this report, we examine the influence of the internal standards ClO_4^- and SO_4^{2-} on the hemoglobin protein structure and the iron spin state and upon the quaternary protein structural transition. We discover significant impact of ClO_4^- and SO_4^{2-} at 0.1 M concentrations, which is more than 2-fold below the concentrations typically used in Raman spectral studies. In this report, we examine two potential Raman internal standards, cacodylic acid and sodium selenate. These species negligibly affect the hemoglobin tertiary or quaternary structure, or the iron spin state. Cacodylic acid is also especially useful since it buffers at physiological pH values (Plumel, 1949; Perutz et al., 1978). We measure the Raman cross sections and the Raman depolarization ratios between 218 and 514.5 nm. The Raman cross sections of cacodylic acid and SeO_4^{2-} in the UV are ca. 5-fold larger than those of ClO_4^- and SO_4^{2-}. We conclude that cacodylic acid and SeO_4^{2-} are superior internal standards for protein structural studies.

Experimental Procedures

Cacodylic acid, sodium selenate, sodium perchlorate, and sodium sulfate were purchased from Aldrich Chemical Co. and used without further purification. Human hemoglobin samples were prepared by standard methods (Antonini & Brunori, 1971). Iron(II) of hemoglobin was oxidized by an excess of $K_3Fe(CN)_6$ which was removed by dialysis against deionized water. Methemoglobin fluoride (met-HbF; R form) and methemoglobin azide (met-HbN_3; R form) were prepared in the presence of 0.1 M NaF or with a 1.5-fold stoichiometry of NaN_3. The R quaternary proteins were converted to their T forms by adding a concentrated buffered solution of inositol hexaphosphate (IHP), at a 4–10-fold excess compared to the heme concentration. The hemoglobin concentrations were determined from the Soret band absorption utilizing known molar absorptivity values (Perutz et al., 1974a). Due to the absorbance changes caused by the high sodium perchlorate and sodium sulfate concentrations, the concentrations of hemoglobin in these samples were specified by the relative dilution of the met-Hb stock solution.

The samples for absorption measurements were prepared at concentrations of 50–100 μM in heme. The solutions were maintained at pH 7.0 by using 30 mM Bis-Tris buffer. However, those samples containing cacodylic acid were self-buffering in the pH 5.2–7.2 range (Plumel, 1949; Perutz et al., 1978). Absorption spectra were measured with a Perkin-Elmer Lambda 9 UV-VIS-NIR spectrophotometer. Far-UV absorption spectra of cacodylic acid at pH 7.0 and sodium selenate in water were obtained after purging the spectrophotometer for 7 h with nitrogen.

The Raman spectrometer is described in detail elsewhere (Asher et al., 1983; Jones et al., 1987). The excitation source utilized a Quanta Ray DCR-2A Nd-YAG laser operated at 20 Hz (pulse width, ca. 4 ns). The 1.06-μm light was frequency-doubled to pump a dye laser. UV light was generated by doubling the dye laser output and mixing it with 1.06-μm YAG fundamental; 260-nm excitation was generated by using a XeCl excimer laser system. The 308-nm fundamental from a Lambda Physik Model EMG 103 excimer laser (200 Hz, 16-ns pulse width) excited a Lambda Physik FL 3002 dye laser, and the dye laser output was frequency-doubled with a β-barium borate doubling crystal. For visible excitation, we used the YAG laser system and mixed the dye laser output with the YAG fundamental to generate 405- and 415-nm light or used an Ar^+ ion laser for 514.5-nm excitation.

An ellipsoidal mirror was used to collect the 90° scattering light. The polarization of the scattered light was randomized by using a crystalline quartz wedge to avoid any polarization efficiency bias of the monochromator gratings. The light was dispersed by a Spex Triplemate monochromator equipped with 1200 groove/mm gratings, and the dispersed light was detected by using a Princeton Applied Research OMA II Model 1420 intensified Reticon detector.

Sodium perchlorate was used as an internal intensity standard for determining the absolute Raman cross sections of the cacodylic acid and SeO_4^{2-} bands; the absolute Raman cross section of the 932 cm^{-1} symmetric stretching mode of perchlorate was previously reported (Dudik et al., 1985). The absolute Raman cross sections of SeO_4^{2-} were determined from relative peak height measurement; the Raman spectral bandwidth observed is dominated by the spectrometer bandpass. We used peak area ratio measurements for cacodylic acid to avoid deconvoluting the 605 cm^{-1} band from the 634 cm^{-1} band. Thus, the reported Raman cross section for cacodylic acid is the sum of both bands. Raman intensities were corrected for the wavelength dependence of the throughput efficiency of the spectrometer, and for the detector sensitivity. Depolarization ratios were measured with a calibrated polacoat analyzer placed prior to the polarization scrambler. The Raman spectra of the cacodylic acid and sodium selenate samples were obtained by using a 1-mm i.d. Suprasil quartz capillary through which the sample was recirculated by a peristaltic pump. The flow rate was sufficient to supply a fresh sample volume between laser pulses. We examined the power flux density dependence of the Raman intensity of cacodylic acid and SeO_4^{2-} to ensure that we maintained the pulse energy flux density below the level which causes Raman saturation or the formation of phototransient bands. The excitation pulse energies were attenuated either by defocusing the laser at the sample or by placing neutral density filters in the beam path. We see no Raman saturation or appearance of photochemical transient Raman bands up to the largest energy flux densities examined (100 mJ/cm^2).

Results and Discussion

The universal use of internal intensity and frequency standards in Raman spectral measurements occurs because relative measurements are much easier than are absolute measurements (Dudik et al., 1985; Blazej & Peticolas, 1980a,b; Trulson & Mathies, 1986). For example, the use of an internal intensity standard permits accurate determination of the Raman cross sections of an analyte, σ_A, from the measured relative intensities:

$$\sigma_A(\nu_0) = \frac{I_A(\nu_0)C_s}{I_s(\nu_0)C_A}\sigma_s(\nu_0) \quad (1)$$

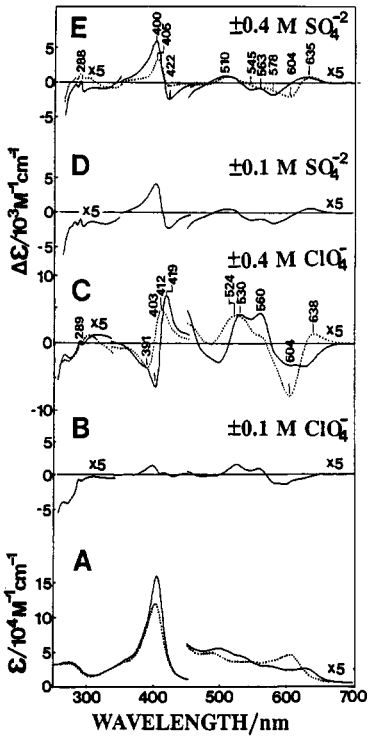

FIGURE 1: (A) Absorption spectra of (solid lines) met-Hb (47.4 μM in heme) and (dotted lines) met-HbF (55.4 μM in heme) in 30 mM Bis-Tris buffer at pH 7.0. Also shown are difference absorption spectra in which spectra A were subtracted from spectra of met-Hb, or of met-HbF (dotted curves) containing (B) 0.1 M ClO_4^-, (C) 0.4 M ClO_4^-, (D) 0.1 M SO_4^{2-}, or (E) 0.4 M SO_4^{2-}. The dashed lines in parts C and E show difference spectra for met-HbF in 30 mM Bis-Tris buffer.

where $\sigma_s(\nu_0)$, C_s, and $I_s(\nu_0)$ are the Raman cross section excited at ν_0, the concentration, and the Raman intensity of the internal standard species, respectively. C_A and $I_A(\nu_0)$ are the concentration and the Raman intensity of the analyte, and ν_0 is the Raman excitation frequency. The experimentally measured Raman intensities are corrected for the throughput efficiencies of the spectrometer and for the self-absorption phenomena present in absorbing samples. This allows accurate determination of the analyte cross sections without requiring knowledge of the incident laser intensity, the solid angle of scattered light collected, or the exact volume of sample probed.

The determination of the analyte cross section is important since these data convey important structural information. This has motivated the recent studies of Raman cross-section excitation profiles of aromatic amino acids in proteins (Ludwig & Asher, 1988; Asher et al., 1986; Asher & Murtaugh, 1988; Sweeney & Asher, 1990; Liu et al., 1989). A major requirement for an internal standard is that it not perturb the analyte spectral data, which requires that it negligibly modify the analyte molecular structure. The internal standard should also undergo no photochemistry or Raman saturation. This generally requires that the analyte not have the absorption bands at the Raman excitation wavelength. Thus, typical internal standards for the ca. 220–260 nm spectral region include species such as SO_4^{2-} and ClO_4^- rather than NO_3^- which absorbs and is photochemically active (Daniels et al., 1968). A potential problem is that the Raman cross sections of SO_4^{2-} and ClO_4^- are small, and the relatively high concentrations required can result in perturbations of the protein structure.

Figure 1 shows the effect of 0.1 and 0.4 M concentrations of ClO_4^- and SO_4^{2-} on the absorption spectra of human aquomethemoglobin (met-Hb) and human methemoglobin fluoride (met-HbF) at pH 7 in a 30 mM Bis-Tris buffer solution. The met-Hb absorption band at 405 nm and the series of bands between 480 and 650 nm derive from heme electronic transitions while the absorption below 300 nm derives mainly from aromatic amino acid π–π^* transitions. The 405-nm Soret bands derives from an in-plane heme $\pi \rightarrow \pi^*$ transition, while the bands between 480 and 650 nm derive both from the α- and β-heme $\pi \rightarrow \pi^*$ transition and also from charge transfer transitions (Eaton & Hochstrasser, 1970; Smith & Williams, 1970; Asher et al., 1977, 1981; Asher, 1981; Perutz et al., 1974a,b, 1978). The absorption spectra of met-Hb are complex due to the fact that the heme exists with the iron in both a high- and a low-spin state. These spin states are in thermal equilibrium with ca. 90% in the high-spin form (Perutz et al., 1974a; Henry et al., 1985). In general, the ca. 600–630-nm derives from the high-spin species while two resolved bands at ca. 570 and 540 nm called the α and β bands derive from the low-spin-state iron (Perutz et al., 1974a).

Addition of 0.1 M ClO_4^- results in spectral changes indicative of both tertiary protein structural changes and also heme spin-state changes. The difference features at ca. 290 and 300 nm are diagnostic of alterations in the absorption spectra of the Trp L_a/L_b 0–0 transitions. The decreased absorbance at ca. 600 nm and the increased absorbance at 530 and 560 nm are indicative of an increased concentration of low-spin-state iron. Only small changes are evident around 400 nm which indicates a similar Soret band for the high- and low-spin heme. A 4-fold increase in the ClO_4^- concentration to 0.4 M results in similar but larger difference spectral features. For example, the 530- and 560-nm features have increased by about 4-fold, while the ca. 600-nm feature only increases ca. 2-fold, but appears to red shift. The Soret band appears to red shift for high (0.4 M) concentrations of ClO_4^-. The Trp absorption spectra changes are essentially identical with those observed at lower ClO_4^- concentrations. It appears that 0.1 M ClO_4^- induces protein tertiary structural changes which are associated with an increased low-spin-state iron. Higher ClO_4^- concentrations result in further spin-state changes and heme absorption red shifts without evidence of additional protein tertiary structural changes.

Figure 1D,E shows that addition of SO_4^{2-} causes comparable spectral changes but these changes are almost the opposite of those caused by ClO_4^- and suggest an increased high-spin-state concentration. In addition, the ca. 300-nm aromatic amino acid absorption changes induced by SO_4^{2-} differ from those caused by ClO_4^-.

Figure 1 also shows the absorption spectrum of the fluoride complex of met-Hb (met-HbF) in 30 mM Bis-Tris buffer. The spectral assignments are similar to those of the aquo complex except that the 600-nm absorption band derives from the high-spin-state (97%) charge transfer band (Perutz et al., 1974a,b; Henry et al., 1985). Addition of 0.1 M ClO_4^- shows essentially the same effect as observed for the aquo complex; an increase is induced in the low-spin population, and a change occurs for the Trp absorption band at ca. 290 nm. Further, an increase in the ClO_4^- concentration to 0.4 M causes a 2–4-fold increase in the bands between 500 and 650 nm (see dotted curve in Figure 1C). The Soret band red shifts in the same manner observed for the met-Hb complex. The higher concentration ClO_4^- data suggest a further shift to low spin; however, the assignment of the positive feature at 638 nm to the low-spin fluoride complex is not completely clear. It is possible that this feature could derive from an increased concentration of the aquo complex, or it could derive from complexation of ClO_4^- to the heme iron. The absorption

spectral changes are similar to but not identical with those observed in the difference absorption spectrum between met-Hb and met-HbF. The 450–700-nm regions are very close, but the Soret band difference spectrum differs, and no changes are clearly evident for the Trp L_a/L_b transition. The formation of an iron–perchlorate complex is unlikely in aqueous solution. Because of the low affinity of perchlorate for iron, perchlorate is easily substituted by other ligands (Kastner et al., 1978; Spiro et al., 1979). Further, as shown below, the structural changes for met-HbF suggest an increase in the concentration of aquo-met-Hb.

In contrast to that observed for the aquo complex, addition of SO_4^{2-} to met-HbF results in an increased concentration of the low-spin species; however, the efficacy of SO_4^{2-} for conversion to low spin is ca. 2-fold less than ClO_4^-. The spectral changes induced by SO_4^{2-} are similar to those observed upon addition of IHP, but the magnitude is less than that observed for the IHP-induced R–T structural change.

In contrast to that in the aquo and fluoride complexes, addition of ClO_4^- to the azide complex of met-Hb (met-HbN_3) results in an increased concentration of the high-spin form, as evident from the increased intensity at 634 nm and the decreased intensities of the ca. 580- and 545-nm low-spin bands. The azide complex is 90% low spin which gives rise to the 571- and 541-nm α and β bands (Perutz et al., 1974a; Henry et al., 1985) and a broad high-spin ca. 630-nm band component (Perutz et al., 1974a). The magnitude of these spectral changes is very similar to that observed for met-HbN_3 upon addition of IHP which shifts the met-HbN_3 quaternary structure from the R to the T form. As observed for met-Hb and met-HbF, the addition of SO_4^{2-} results in an increase in the high-spin concentration, but the efficacy of SO_4^{2-} is less than that of ClO_4^-.

In contrast to the similarity for met-HbN_3 for the ClO_4^-, SO_4^{2-} and IHP-induced absorption spectral changes, significant differences exist for the absorption spectral changes induced for met-HbF between ClO_4^- and SO_4^{2-} and IHP. For example, the difference spectra suggest that the 600-nm high-spin charge transfer band red shifts upon IHP addition and the spectral alteration in the ca. 290-nm spectral region seems to be much sharper.

It appears that both SO_4^{2-} and ClO_4^- change the energy difference between the two spin states for met-Hb, met-HbF and met-HbN_3. However, the changes induced for met-HbF by ClO_4^- differ from those observed upon IHP addition. As previously noted, high ionic strengths decrease the spectral changes induced by IHP, presumably due to the decreased IHP binding affinity at the higher ionic strengths (Perutz et al., 1974b). In fact, for met-HbN_3, no IHP-induced spectral changes occur in the presence of 0.1 M ClO_4^- or SO_4^{2-} (not shown). There is evidence for a SO_4^{2-} binding site in hemoglobin (Ladner et al., 1977).

Figure 2 shows Soret-excited (405 nm) heme resonance Raman spectra of met-Hb and met-HbF with and without addition of ClO_4^- and SO_4^{2-}. The most strongly Soret-enhanced vibrations derive from heme in-plane ring vibrations (Asher et al., 1981; Asher, 1981; Henry et al., 1985; Spiro & Strekas, 1974; Spiro et al., 1979; Abe et al., 1978; Shelnutt et al., 1979). The dominant band at ca. 1370 cm^{-1} is the ν_4 oxidation state sensitive band; this band has recently also been shown to be modestly sensitive to globin structure (Henry et al., 1985). The Raman bands at ca. 1510 cm^{-1} and ca. 1580 cm^{-1} are the ν_3 and ν_2 of the low-spin species, while the ca. 1480 cm^{-1} and the ca. 1560 cm^{-1} bands derive from the high-spin species (Asher et al., 1981; Asher, 1981; Henry et al., 1985; Spiro & Strekas, 1974; Spiro et al., 1979; Shelnutt et al., 1979). The 1623 cm^{-1} bands derive mainly from the heme vinyl stretching vibration.

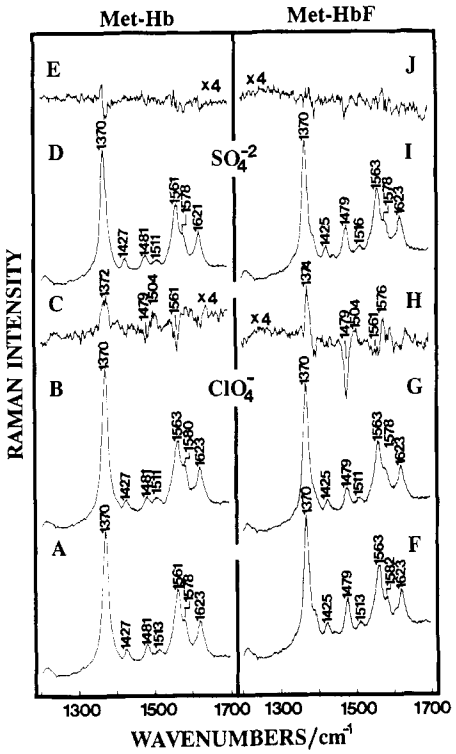

FIGURE 2: Soret-excited resonance Raman spectra of (A) met-Hb, (B) met-Hb with 0.4 M perchlorate ion, (C) spectrum B – A, (D) met-Hb with 0.4 M sulfate ion, (E) spectrum D – A, (F) met-HbF, (G) met-HbF with 0.4 M ClO_4^-, (H) spectrum G–F, (I) met-HbF with 0.4 M SO_4^{2-}, and (J) spectrum I – F.

For met-Hb, the Figure 2C Raman difference spectrum shows that addition of 0.4 M ClO_4^- results in a decreased intensity for the high-spin bands at 1479 and 1561 cm^{-1} and an increased intensity for the low-spin band at 1504 cm^{-1}. The broad band at ca. 1580 cm^{-1} is also indicative of an increase of the low-spin concentration. The individual spectra were scaled such that the vinyl band intensities were identical between spectra. The small increase in the ν_4 intensity presumably derives from the small Soret band shift upon ClO_4^- addition. Addition of 0.4 M SO_4^{2-} shows, as expected, a much smaller effect, and no spin-state changes are clearly evident.

For met-HbF, addition of ClO_4^- results in a ca. 30% decrease in the high-spin 1479 cm^{-1} band and a smaller increase in the low-spin 1504 cm^{-1} band. A decreased intensity occurs for the high-spin 1563 cm^{-1} band which is compensated by an increased low-spin 1576 cm^{-1} band. As previously observed in the absorption difference spectrum (Figure 2J), 0.4 M SO_4^{2-} causes a similar but significantly smaller Raman spectral change. The large 1479 cm^{-1} band intensity change may suggest that part of the high-spin to low-spin conversion in met-HbF derives from a decreased affinity for fluoride and an increased met-Hb concentration; the high-spin 1479 cm^{-1} band intensity in met-Hb is much less than that for met-HbF, even after accounting for the met-Hb high-spin concentration decrease. Presumably, the presence of ClO_4^- also affects the met-HbF Raman spectra to result in a spectrum close to that of met-Hb.

We have examined other species as potential Raman internal intensity standards and find that cacodylic acid and SeO_4^{2-} are excellent candidates; they have high Raman cross sections and few bands to interfere with studies of the analyte and do not undergo photochemistry with the pulse energy flux density

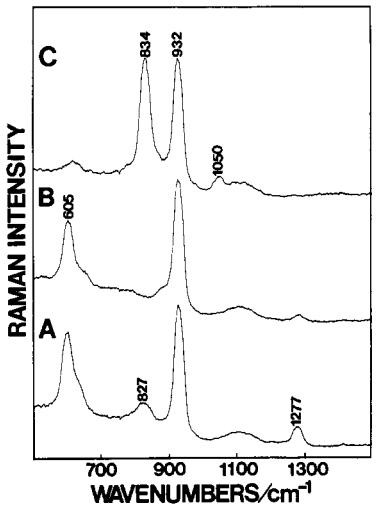

FIGURE 3: Raman spectra at 220-nm excitation of (A) 0.1 M cacodylic acid, pH 7.0, (B) 0.1 M cacodylic acid, pH 2.0, and (C) 0.1 M selenate. Spectral band-pass is 29 cm^{-1}. The 932 cm^{-1} band derives from 0.5 M ClO_4^-.

excitation condition used in typical UV resonance Raman measurements. Further, they do not visibly affect the met-Hb protein structure or iron spin state.

The *IHP-induced* absorption spectral changes for met-HbF in 30 mM Bis-Tris buffer with either 0.1 M cacodylic acid or SeO_4^{2-} are essentially identical with those observed in 30 mM Bis-Tris buffer solution. This indicates no interaction of these species with the protein. We also observe negligible absorption spectral changes for met-Hb and met-HbF in 30 mM Bis-Tris buffer induced by addition of these species. Thus, these ions are useful as noninteractive internal standards.

Figure 3 shows the 220-nm excited Raman spectrum of cacodylic acid, $(CH_3)_2As(O)OH$, at pH 7 and 2, and of SeO_4^{2-}. The 605 and 634 cm^{-1} cacodylic acid Raman band doublet derives from the symmetric and asymmetric stretching modes of As–C linkage, respectively (Glundler et al., 1974; Vansant et al., 1974). The bandshape and Raman cross sections of the cacodylic acid 605 and 634 cm^{-1} bands are pH dependent; the pK_a is 6.19. At low pH values, where the cacodylic acid is protonated, these bands show an increased intensity on the high-frequency side of the 605/634 cm^{-1} doublet. The Raman cross section of this doublet, which we determine by an area measurement over both components, decreases by 10% for the protonated form to 1.3×10^{-27} $cm^2/(mol \cdot sr)$ at 239-nm excitation compared to that observed for the unprotonated form. Figure 3C shows the 220-nm Raman spectrum of SeO_4^{2-}. The 834 cm^{-1} band derives from the symmetric stretching vibration (Nakamoto, 1978). The depolarization ratios for the cacodylic acid 605 cm^{-1} band and the SeO_4^{2-} 834 cm^{-1} bands are 0.18 ± 0.02 and 0.05 ± 0.02 for 514.5-nm excitation and 0.18 ± 0.02 and 0.05 ± 0.02 for 220-nm excitation, respectively. The 220-nm excitation Raman cross sections of cacodylic acid and SeO_4^{2-} are ca. 5-fold larger than those of SO_4^{2-} and ClO_4^-, and thus, these species can be used as internal intensity standards at 5-fold lower concentrations than can ClO_4^- and SO_4^{2-}.

Figure 4A shows the Raman excitation profile cross-section dispersion of the 605/634 cm^{-1} doublet of cacodylic acid at pH 7, while Figure 4B shows the cross-section dispersion of SeO_4^{2-}. The cross sections monotonically increase as excitation occurs further into the UV. Table I lists the Raman cross sections of these species at various excitation wavelengths. The dispersions of the preresonance Raman cross sections are often modeled by using the modified Albrecht *A*-term expression

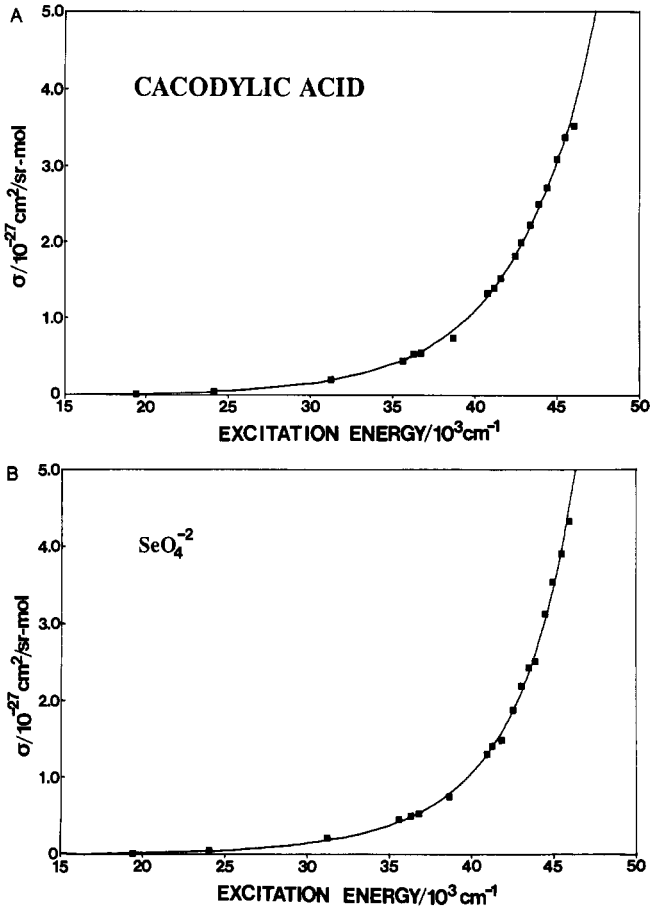

FIGURE 4: (A) Differential Raman cross-section excitation profile of the cacodylic acid 605/634 cm^{-1} doublet from 514.5 to 218 nm. The solid curve represents the best fit of the data to the modified Albrecht *A* term (see text for details). (B) Differential Raman cross-section excitation profile of the selenate 834 cm^{-1} band between 514.5 and 218 nm. The solid curve is the best fit of the data to the modified Albrecht *A* term.

Table I: Differential Raman Cross Sections for Cacodylic Acid 605 and 634 cm^{-1} Doublet Bands and for the SeO_4^{2-} 834 cm^{-1} Band[a]

λ_0 (nm)	cacodylic acid	SeO_4^{2-}
514.5	28	18
415	58	55
320	210	220
280	430	450
260	700	720
240	1500	1400
230	2300	2400
225	2700	3100
220	3300	3900
218	3500	4300

[a] Cross section units are $\times 10^{-30}$ $cm^2/(sr \cdot mol)$.

(Tang & Albrecht, 1978; Albrecht, 1960; Albrecht & Hutley, 1971; Dudik et al., 1985):

$$\sigma_R(\nu_0) = K_1\nu_0(\nu_0 - \nu_{mn})^3 \left[\frac{\nu_e^2 + \nu_0^2}{(\nu_e^2 - \nu_0^2)^2} + K_2 \right]^2 \quad (2)$$

where K_1 and K_2 are constants. K_1 is independent of the excitation frequency and depends on the oscillator strength of the excited state and on the coupling between the vibration and the electronic transition. When $K_2 = 0$, eq 2 corresponds to the simple *A*-term expression, and the intensity dispersion is modeled as being dominated by a single electronic transition state. K_2 is a phenomenological term that permits the con-

Table II: Albrecht *A*-Term Fitting Parameters for the Raman Cross Section of Cacodylic Acid and SeO_4^{2-}

	simple *A* term		modified *A* term		
	K_1[a]	ν_e[b]	K_1[a]	K_2[c]	ν_e[b]
cacodylic acid	2.54 ± 10^{-27}	131	2.46×10^{-27}	1.27×10^{-13}	132
SeO_4^{2-}	1.12×10^{-27}	145	1.54×10^{-28}	5.76×10^{-10}	162

[a] Units: $cm^2/(sr \cdot mol)$. [b] Units: nm. [c] Units: $(cm^{-1})^2$.

tribution of an additional higher energy transition to the Raman cross section. The Raman cross-section data of Figure 4A,B were fitted to eq 2 by a nonlinear squares fit, and the resulting transition energies and K_1 values calculated by the simple and modified *A*-term fits are listed in Table II. The solid lines in Figure 4A,B, which are best fits to the modified *A*-term expression, accurately model the experimental cross-section dispersion. The preresonance state calculated by the simple *A* term occurs at 76 000 cm^{-1} (131 nm) for cacodylic acid and at 69 000 cm^{-1} (145 nm) for SeO_4^{2-}. The modified *A* term shows a similar transition frequency for cacodylic acid at 75 800 cm^{-1} (132 nm), but the transition frequency shifts to lower energy for SeO_4^{2-} to 61 700 cm^{-1} (162 nm). Absorption spectra show a maximum at 182 nm for cacodylic acid and at 184 nm for SO_4^{2-}. To our knowledge, no clear assignment of the 182-nm cacodylic acid electronic transition exists. In the case of SeO_4^{2-}, a charge transfer transition to solvent occurs at ca. 182 nm (Blandamer & Fox, 1971). Obviously, transitions further in the UV dominate the observed preresonance enhancement of cacodylic acid and SeO_4^{2-}.

Our calculated cacodylic acid preresonance frequency is similar to that of Trulson and Mathies (1986) of 83 000 cm^{-1} (120 nm). However, our value differs from that assumed previously by Blazej and Peticolas (1980a,b) from the absorption spectrum. The increased Raman cross section of cacodylic acid and SeO_4^{2-} compared to ClO_4^- and SO_4^{2-} results from their decreased preresonance transition frequencies compared to the ca. 120 000 cm^{-1} transition frequencies for ClO_4^- and SO_4^{2-} (Dudik et al., 1985).

Our measured UV Raman cross section of cacodylic acid at 239 nm compares favorably to that previously measured by Trulson and Mathies (1986). They measure a *total* Raman cross section, σ_R (integrated over 4π sr), of 13×10^{-27} $cm^2/(mol \cdot sr)$ for sodium cacodylate (pH unknown). Given the measured depolarization ratio of 0.18, the differential Raman cross section is calculated from their result to be

$$\sigma = \frac{d\sigma_R}{d\Omega} = \frac{3}{8\pi}\left(\frac{1+\rho}{1+2\rho}\right)\sigma_R = 1.33 \times 10^{-27}\ cm^2/(sr \cdot mol) \quad (3)$$

which is 11% less than the 1.5×10^{-27} $cm^2/(sr \cdot mol)$ value we measure. In contrast, our differential cross section of 0.028 $\times 10^{-27}$ $cm^2/(sr \cdot mol)$ measured at 514.5 nm is 40% greater than their differential Raman cross section value of 0.019 $\times$ 10^{-27} $cm^2/(sr \cdot mol)$.

Conclusions

Cacodylic acid and SeO_4^{2-} are superior UV resonance Raman intensity standards for heme protein studies. Studies of human met-Hb derivatives indicate that SeO_4^{2-} and cacodylic acid insignificantly perturb the absorption spectral signatures of the protein tertiary structure, and do not perturb the R $\rightarrow$ T structural transition induced by the allosteric effector, IHP. This is in contrast to internal standards such as ClO_4^- and SO_4^{2-} which cause changes in the Trp absorption bands and change the heme iron spin state. In addition, ClO_4^- and SO_4^{2-} suppress the met-HbF and met-HbN_3 quaternary conversion induced by IHP. Finally, cacodylic acid and SeO_4^{2-} have UV Raman cross sections ca. 5-fold greater than ClO_4^- and SO_4^{2-}, and thus can be used at 5-fold lower concentrations.

Registry No. Na_2SeO_4, 13410-01-0; $NaClO_4$, 7601-89-0; Na_2SO_4, 7757-82-6; cacodylic acid, 75-60-5.

References

Abe, M., Kitakawa, T., & Kyogoku, Y. (1978) *J. Chem. Phys. 69*, 4526.

Albrecht, A. C. (1960) *J. Chem. Phys. 34*, 1476.

Albrecht, A. C., & Hutley, M. C. (1971) *J. Chem. Phys. 55*, 4438.

Antonini, E., & Brunori, M. (1971) in *Hemoglobin and Myoglobin in Their Reactions with Ligands*, Chapter 1, p 1, North-Holland Publishing Co., Amsterdam.

Asher, S. A. (1981) *Methods Enzymol. 76*, 371.

Asher, S. A. (1988) *Annu. Rev. Phys. Chem. 39*, 537.

Asher, S. A., & Murtaugh, J. L. (1988) *App. Spectrosc. 42*, 83.

Asher, S. A., Vickery, L. E., Schuster, T. M., & Sauer, K. (1977) *Biochemistry 16*, 5849.

Asher, S. A., Adams, M. L., & Schuster, T. M. (1981) *Biochemistry 20*, 3339.

Asher, S. A., Johnson, C. R., & Murtaugh, J. (1983) *Rev. Sci. Instrum. 54*, 1657.

Asher, S. A., Ludwig, M., & Johnson, C. R. (1986) *J. Am. Chem. Soc. 108*, 3186.

Blandamer, M. J., & Fox, M. F. (1970) *Chem. Rev. 70*, 59.

Blazej, D. C., & Peticolas, W. L. (1980a) *Proc. Natl. Acad. Sci. U.S.A. 74*, 2639.

Blazej, D. C., & Peticolas, W. L. (1980b) *J. Chem. Phys. 72*, 3134.

Daniels, M. D., Meyers, R. V., & Belardo, E. V. (1968) *Symp. Inorg. Photochem. 72*, 389.

Dudik, J. M., Johnson, C. R., & Asher, S. A. (1985) *J. Chem. Phys. 82*, 1732.

Eaton, W. A., & Hochstrasser, R. M. (1970) *J. Chem. Phys. 49*, 985.

Grundler, H.-V., Schumann, H. D., & Steger, E. (1974) *J. Mol. Struct. 21*, 149.

Harada, I., & Takeuchi, H. (1986) in *Spectroscopy of Biological Systems* (Clark, R. J. H., & Hester, R. E., Eds.) p 113, John Wiley & Sons, Chichester.

Harada, I., Yamagishi, T., Uchida, K., & Takeuchi, H. (1990) *J. Am. Chem. Soc. 112*, 2443.

Harmon, P. A., Teraoka, J., & Asher, S. A. (1990) *J. Am. Chem. Soc. 112*, 8789.

Henry, E. R., Rousseau, D. L., Hopfield, J. J., Noble, R. W., & Simon, S. R. (1985) *Biochemistry 24*, 5907.

Johansson, L. (1974) *Coord. Chem. Rev. 12*, 241.

Jones, C. M., DeVito, V. L., Harmon, P. A., & Asher, S. A. (1987) *Appl. Spectrosc. 41*, 1268.

Kaminaka, S., Ogura, T., & Kitakawa, T. (1990) *J. Am. Chem. Soc. 112*, 23.

Kastner, M. E., Scheidt, W. R., Mashiko, T., & Reed, C. A. (1978) *J. Am. Chem. Soc. 100*, 666.

Kubasek, W. L., Hudson, B., & Peticolas, W. L. (1985) *Proc. Natl. Acad. Sci. U.S.A. 82*, 2369.

Ladner, R. C., Heidner, E. J., & Perutz, M. F. (1977) *J. Mol. Biol. 114*, 385.

Larkin, P. J., Teraoka, J., & Asher, S. A. (1990a) *Biochemistry* (submitted for publication).

Larkin, P. J., Gustafson, W. G., & Asher, S. A. (1990b) *J. Chem. Phys.* (submitted for publication).

Li, B., & Myers, A. B. (1990) *J. Phys. Chem. 94*, 4051.
Liu, G.-Y., Grygon, C. A., & Spiro, T. G. (1989) *Biochemistry 28*, 5046.
Ludwig, M., & Asher, S. A. (1988) *J. Am. Chem. Soc. 110*, 1005.
Nakamoto, K. (1978) in *IR and Raman Spectra of Inorganic and Coordination Compounds*, p 103, John Wiley & Sons, New York.
Perutz, M. F., Heidner, E. J., Ladner, J. E., Beetlestone, J. G., Ho, C., & Slade, E. F. (1974a) *Biochemistry 13*, 2187.
Perutz, M. F., Fersht, A. R., Simon, S. R., & Roberts, G. C. K. (1974b) *Biochemistry 13*, 2174.
Perutz, M. F., Sanders, J. K. M., Chenery, D. H., Noble, R. W., Pennelly, R., Fung, L. W.-M., Ho, C., Giannini, I., Porschke, D., & Winkler, H. (1978) *Biochemistry 17*, 3640.
Plumel, M. (1949) *Bull. Soc. Chim. Biol. 30*, 129.
Shelnutt, J. A., Rousseau, D. L., Friedman, J. M., & Simon S. R. (1979) *Proc. Natl. Acad. Sci. U.S.A. 76*, 4409.
Smith, D. W., & Williams, R. J. P. (1970) *Struct. Bonding (Berlin) 7*, 1.
Song, S., & Asher, S. A. (1990) *J. Am. Chem. Soc.* (in preparation).
Spiro, T. G., & Strekas, T. C. (1974) *J. Am. Chem. Soc. 96*, 338.
Spiro, T. G., Strong, J. D., & Stein, P. (1979) *J. Am. Chem. Soc. 101*, 2648.
Su, C., Park, Y. D., Liu, G.-Y., & Spiro, T. G. (1989) *J. Am. Chem. Soc. 111*, 3457.
Sweeney, J. A., & Asher, S. A. (1990) *J. Phys. Chem. 94*, 4784.
Sweeney, J. A., Harmon, P. A., Asher, S. A., Hutnik, C. M., & Szabo, A. G. (1990) *J. Am. Chem. Soc.* (submitted for publication).
Tang, J., & Albrecht, A. C. (1970) in *Raman Spectroscopy, Theory and Practice* (Szymanski, H. A., Ed.) Vol. II, p 33, Plenum, New York.
Trulson, M. O., & Mathies, R. A. (1986) *J. Chem. Phys. 84*, 2068.
Vansant, F. K., van der Veken, B. J., & Herman, M. A. (1974) *Spectrochim. Acta A 30A*, 69.

Age-Dependent Accumulation of N^{ϵ}-(Carboxymethyl)lysine and N^{ϵ}-(Carboxymethyl)hydroxylysine in Human Skin Collagen†

John A. Dunn,‡ David R. McCance,§ Suzanne R. Thorpe,‡ Timothy J. Lyons,§ and John W. Baynes*,‡,∥

Department of Chemistry and School of Medicine, University of South Carolina, Columbia, South Carolina 29208, and Sir George E. Clark Metabolic Unit, Royal Victoria Hospital, Belfast BT12 6BA, Northern Ireland

Received October 11, 1990

ABSTRACT: N^{ϵ}-(Carboxymethyl)lysine (CML) is formed on oxidative cleavage of carbohydrate adducts to lysine residues in glycated proteins in vitro [Ahmed et al. (1988) *J. Biol. Chem. 263*, 8816–8821; Dunn et al. (1990) *Biochemistry 29*, 10964–10970]. We have shown that, in human lens proteins in vivo, the concentration of fructose–lysine (FL), the Amadori adduct of glucose to lysine, is constant with age, while the concentration of the oxidation product, CML, increases significantly with age [Dunn et al. (1989) *Biochemistry 28*, 9464–9468]. In this work we extend our studies to the analysis of human skin collagen. The extent of glycation of insoluble skin collagen was greater than that of lens proteins (4–6 mmol of FL/mol of lysine in collagen versus 1–2 mmol of FL/mol of lysine in lens proteins), consistent with the lower concentration of glucose in lens, compared to plasma. In contrast to lens, there was a slight but significant age-dependent increase in glycation of skin collagen, 33% between ages 20 and 80. As in lens protein, CML, present at only trace levels in neonatal collagen, increased significantly with age, although the amount of CML in collagen at 80 years of age, ~1.5 mmol of CML/mol of lysine, was less than that found in lens protein, ~7 mmol of CML/mol of lysine. The concentration of N^{ϵ}-(carboxymethyl)hydroxylysine (CMhL), the product of oxidation of glycated hydroxylysine, also increased with age in collagen, in parallel with the increase in CML, from trace levels at infancy to ~5 mmol of CMhL/mol of hydroxylysine at age 80. Thus, accumulation of *N*-(carboxymethyl) amino acids appears to be a general feature of the aging of long-lived proteins by glycation and oxidation reactions.

Glycation (nonenzymatic glycosylation) is a posttranslational modification of proteins resulting from reaction of glucose with amino groups in protein (Baynes et al., 1989). The ϵ-amino group of lysine residues is the primary site of modification of most proteins, resulting in the formation of the Amadori compound fructose–lysine (FL)[1] (Figure 1). We reported previously that FL may be cleaved oxidatively to form N^{ϵ}-(carboxymethyl)lysine (CML) residues in proteins in vitro (Ahmed et al., 1986, 1988) and showed recently (Dunn et al.,

† This work was supported by Research Grant DK-19971 from the National Institute of Diabetes and Digestive and Kidney Diseases.
* To whom correspondence should be addressed at the Department of Chemistry, University of South Carolina.
‡ Department of Chemistry, University of South Carolina.
§ Royal Victoria Hospital.
∥ School of Medicine, University of South Carolina.

[1] Abbreviations: CMhL, N^{ϵ}-(carboxymethyl)hydroxylysine; CML, N^{ϵ}-(carboxymethyl)lysine; GC/MS, gas chromatography–mass spectrometry; FL, N^{ϵ}-(1-deoxyfructos-1-yl)-L-lysine (fructose–lysine); Hyl, hydroxylysine; SIM, selected-ion monitoring; TFAME, trifluoroacetyl methyl ester.

0006-2960/91/0430-1205$02.50/0